Tracer Technologies for Hydrological Systems (Proceedings of a Boulder Symposium, July 1995). IAHS Publ. no. 229, 1995.

Isotopic analysis of hydrologic processes in a small semiarid catchment

PADINARE V. UNNIKRISHNA
Department of Civil and Environmental Engineering, Utah State University, Logan, Utah 84322-8200, USA

JEFFREY J. MCDONNELL
College of Environmental Science and Forestry, State University of New York (SUNY), Syracuse, New York 13210, USA

DAVID G. TARBOTON
Department of Civil and Environmental Engineering, Utah State University, Logan, Utah 84322-8200, USA

CAROL KENDALL
United States Geological Survey, Menlo Park, California 94025, USA

Abstract In an effort to better understand the dominant flow processes in semiarid systems, an experiment was conducted in a highly instrumented 26 ha catchment in Idaho, USA. Snowmelt from deep snow drifts constitutes the main input into the basin. Subsurface geology consists of four basaltic layers underlying a soil layer – fractured basalt, semi-dense basalt, altered basalt and dense basalt. A total of 1600 water samples of precipitation, snowmelt, streamflow and groundwater were collected and analysed for $\delta^{18}O$. Isotopic data indicate that snowmelt flow to the stream is mainly through the altered basalt layer, largely bypassing the fractured basalt zone above. Within the altered basalt zone, isotopically enriched snowmelt mixes sequentially with large volumes of previously stored water. Tracer compositions indicated lack of active exchange of water between the geologic zones. Implications of findings for water balance modelling based on topography are discussed.

INTRODUCTION

Several isotope-based studies have investigated flow mechanisms and runoff processes in small catchments (Sklash & Farvolden, 1979; McDonnell, 1990; Harris *et al.*, 1995). Study sites have included a wide range of hydrogeologic environments in primarily humid areas. In most cases, clear separation of runoff source areas has been achieved on the time-scale of rainfall events (Pearce *et al.*, 1986) and snowmelt inputs (Wels *et al.*, 1993). A recent review by Buttle (1994) demonstrates that while many hydrologic regimes have been studied, few of the research catchments have been located in semiarid or arid regions.

Investigations of flow processes in semiarid regions are problematic because, in most cases, flow is highly irregular and streams are ephemeral. In mid-latitude semiarid systems, much of the runoff derives from seasonal snowmelt. In such systems, catch-

ment storage and evapotranspirational loss are the dominant influences on streamflow. Furthermore, water flow pathways are difficult to determine, due to periodic extremes in catchment moisture deficit. The present study was undertaken to gain a better understanding of runoff production, source areas and flow paths in a semiarid environment. Specific questions addressed in this paper are: (1) How is groundwater recharged during snowmelt? (2) How do flow paths determine streamflow isotopic composition? (3) What are the implications of (1) and (2) for hydrologic modelling in semiarid catchments?

STUDY AREA

The Reynolds Creek Experimental Watershed is intensively monitored as a long term research site by the Agricultural Research Service (ARS). The watershed covers an area of 234 km^2 and ranges in elevation from 1100 to 2250 m. Annual precipitation ranges from 240 mm at the lower elevations to 1130 mm at the upper elevations. The Upper Sheep Creek is a small 26 ha first-order sub-basin with an elevation range of 1840 to 2036 m. Streamflow is ephemeral and occurs mainly in response to snowmelt in May and June. Vegetation is primarily sagebrush with local groves of aspen. A detailed description of the area is given in Flerchinger *et al.* (1992). The topography of Upper Sheep Creek is shown in Fig. 1, overlain with a 30 m x 30 m grid to reference instrument locations by transect number and row letter. The northeast facing slopes are characterized by the formation of deep snow drifts due to the southwesterly winter storms. The main drift typically extends from I5 to K17 (Fig. 1), approximately parallel to the basin boundary.

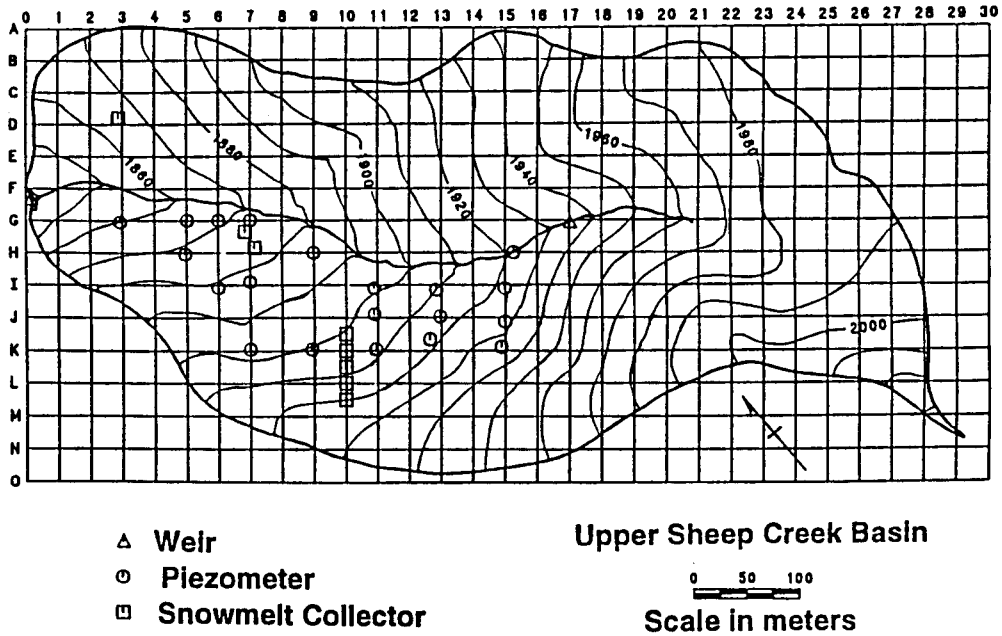

Fig. 1 Upper Sheep Creek basin topography and instrumentation.

Geology

Several studies have investigated the geology of the Upper Sheep Creek basin. Winkelmaier (1987) classified the subsurface into five vertical zones (Fig. 2) using slug test data. Zone 1 is a dark loam soil and is thickest between K8 and M8 and between I16 and L16. Zone 2 consists of fractured basalt. Zone 3 is dense to semi-dense basalt. Extensive altered basalt constitutes Zone 4. The lowermost Zone 5 consists of very hard, dark grey basalt bedrock. Approximate hydraulic conductivity (K) values from slug tests are also shown.

Mock (1988) delineated hydro-stratigraphy and bedrock topography based on seismic refraction surveys. Stevens (1991) conducted an extensive geophysical survey of the basin using a variety of techniques such as magnetic surveys, very low frequency electromagnetic surveys, surface resistivity studies and seismic refraction methods. These studies confirmed the existence of the four distinct and laterally extensive basalt layers covering the entire drainage. The geologic zones were found to be symmetric on both sides of the stream and are thought to be the result of basalt flows deposited over an irregular surface and brought to their present position due to structural activity (Stevens, 1991). The geophysical methods did not identify any sizeable fractures. Resistivity data (Stevens, 1991) showed hydraulic conductivity values of 1.97e-6 m s^{-1} in the altered basalt zone near H8 decreasing rapidly to less than 1.16e-7 m s^{-1} in the lower portion of the basin below transect 5.

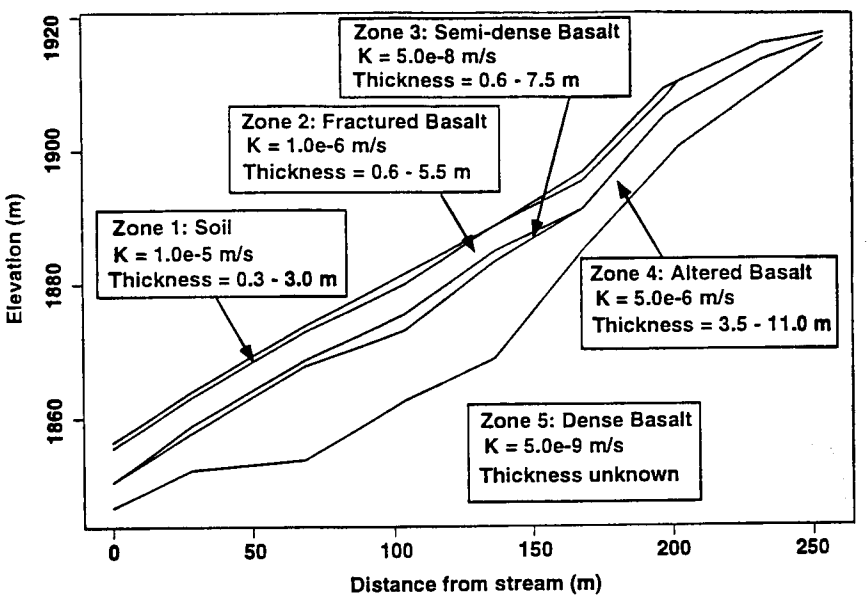

Fig. 2 Geologic cross section from stream near F5 to basin boundary at M7 (Flerchinger *et al.*, 1992).

MEASUREMENTS

Upper Sheep Creek is intensively monitored as part of the ongoing ARS research programme. Field instrumentation consists of precipitation gauges, snowmelt collectors,

piezometers, weirs and meteorological instrumentation towers. Hourly snowmelt was recorded by tipping bucket collectors located at sites D3, G6 and J10. Locations D3 and G6 are influenced by snow cover on the south and northeast facing slopes respectively. The collectors at D3 monitor an area with shallow soil covered by sparse vegetation. Collectors at J10 monitor the main drift snowmelt. Hourly piezometric head in the geologic zones is monitored by pressure transducers in a network of 36 piezometers at 20 locations (Fig. 1). Most of the piezometers monitor the permeable altered basalt zone. A total of six weirs located at the basin outlet and near transects 5, 8, 11, 14 and 17 continuously record streamflow.

Intensive field sampling was conducted during the winter and snowmelt season of 1993. A total of 1600 daily, and in some cases, hourly water samples of snowmelt, rainfall, groundwater and streamflow were collected. An automatic Manning sampler was used to collect six-hourly samples at the lower weir throughout the period of streamflow for isotopic composition analysis.

RESULTS

The study year 1993 had above average snowfall but was preceded by an extremely dry year. Snowmelt and rainfall input to the basin with $\delta^{18}O$ values at D3, G6 and J10 are shown in Fig. 3. Snow cover persisted on the south facing slope until March 24 and on the northeast facing slope until April 16. Snowmelt at D3 and G6 indicative of basinwide melt occurred mainly in March. During this period, active snowmelt also occurred from the drift between March 17 and 28 with a maximum rate of 47.4 mm day^{-1}. After this basinwide snowmelt, isolated drift snowmelt began on May 1 and lasted until the drift completely disappeared around May 20. Major drift snowmelt occurred between May 6 and 20 with a maximum rate of 42.4 mm day^{-1}.

Basin hydrometric response to spring snowmelt

The piezometric response observed in the lower four geologic zones indicated the presence of multiple water tables. Within the altered basalt zone most piezometers began responding at the end of general snowmelt and peaked during the second half of May when drift snowmelt was maximum. Piezometer heads receded thereafter until September. Piezometer responses at G7, H7, I7, and J7 began on March 24, April 19, May 12 and May 14 respectively. This suggests gradual filling up of the altered basalt zone from the stream in the upslope direction with the progress of drift snowmelt. During peak drift snowmelt, confined flow conditions also became established at several locations within this zone. In the other three geologic zones, piezometer responses were less significant, but mostly matched the timing of the altered basalt response.

Streamflow in the basin did not begin until the non-drift snow cover had disappeared, with flow commencing at all six weirs on May 3. On May 17, a spring at transect 4 also started discharging and continued until the end of June. Streamflow at the outlet weir ceased in mid-July. Streamflow at transects 5, 8, 11, 14 and 17 stopped on June 22, May 27, June 28, May 29 and June 22 respectively.

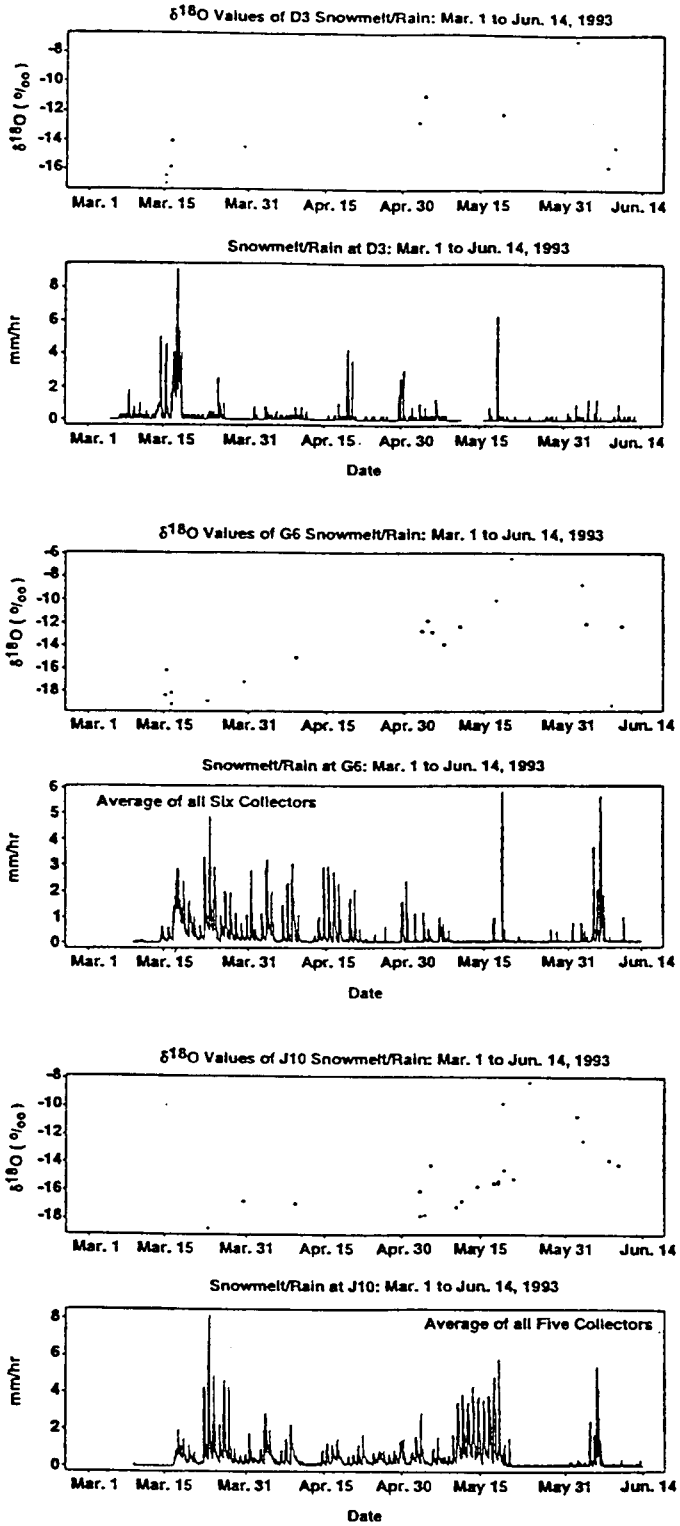

Fig. 3 Snowmelt rates and corresponding $\delta^{18}O$ values at D3, G6 and J10 locations.

Isotope tracer variation

Snowmelt $\delta^{18}O$ compositions ranged from -19.30 to $-6.40‰$ and showed significant enrichment in $\delta^{18}O$ (less negative values) towards the end of the melt period at all three measurement sites (Fig. 3). During major snowmelt events, the isotopic composition of snowmelt samples were more enriched than that of other basin waters. This enabled effective flow tracing and interpretation of subsurface flow processes.

Variations in $\delta^{18}O$ along the stream channel for May 18, May 24, June 8 and June 23 are shown in Fig. 4. In this figure, transect 0 is the basin outlet and successive transect numbers indicate 30 m increments upstream. For the entire duration of streamflow, $\delta^{18}O$ showed steady enrichment from $-18.00‰$ at the uppermost weir 6 to $-17.20‰$ at the outlet. A measurable enrichment of $\delta^{18}O = 0.5‰$ was seen throughout May and June from transects 14 to 11. Below transect 11, $\delta^{18}O$ enrichment was also observed over time and was most prominent towards the end of the drift melt period. During the initial period of streamflow, spring water at transect 4 had $\delta^{18}O$ values around $-17.00‰$ as compared to streamflow values of $-17.40‰$.

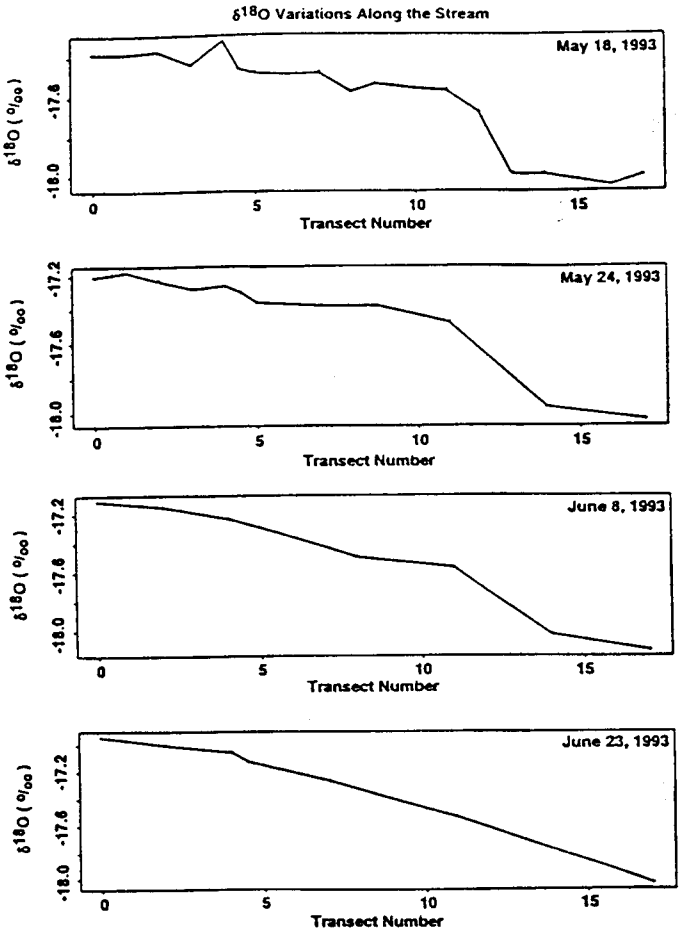

Fig. 4 $\delta^{18}O$ variations along the stream channel.

Before general snowmelt began, several piezometers were dry throughout the basin. Pre-melt $\delta^{18}O$ within the altered basalt zone at H13 and H15 were −18.15‰ and −17.14‰ respectively, while the dense basalt $\delta^{18}O$ at J11 was −12.75‰. Isotopic compositions of subsurface waters revealed distinct ranges specific to both location in the basin and geologic zone. Values for groundwater $\delta^{18}O$ in the various geologic zones on May 21 when snowmelt $\delta^{18}O$ from the main drift was −15.20‰ are shown in Fig. 5. This schematic represents a geologic cross section from the stream along transects 6 and 7 up to *K* (as in Fig. 1) and will be referred to in the following discussion. The structural high shown is a local peak in the semi-dense basalt zone as identified by Stevens (1991) between H16 and I16, J11 and K11, J8 and K8. The fractured (zone 2) and semi-dense basalt (zone 3) at locations K7, I6 and G6 had $\delta^{18}O$ ranges of −17.60 to −17.05‰, −17.90 to −17.10‰ and −17.40 to −17.00‰, respectively throughout May and June. The isotopic composition at midslope location I6 was generally more depleted in $\delta^{18}O$. However, neither of these locations reflected the enriched $\delta^{18}O$ of the snowmelt input. This depletion (larger negative values) of $\delta^{18}O$ composition in zones 2 and 3 is clearly seen in Fig. 5.

Evidence of the main drift snowmelt $\delta^{18}O$ is found in the isotopic composition of the altered basalt (zone 4) at the toe of the drift (Fig. 5). The ranges in $\delta^{18}O$ composition of water samples from the altered basalt at locations J7, I7, H7 and G7 were −15.60 to −15.26‰, −15.70 to −15.55‰, −16.85 to −16.60‰ and −17.50 to −16.85‰, respectively throughout May and June. Isotope values appeared distinct at each location and show progressive depletion of altered basalt zone $\delta^{18}O$ towards the stream (Fig. 5) reflecting the infiltration of recent snowmelt ($\delta^{18}O$ = −15.20‰).

Piezometers at I6 and J11 in the dense basalt (zone 5) showed $\delta^{18}O$ ranges between −16.45 to −16.25‰ and −16.95 to −16.65‰, respectively throughout May and June. By March 23, $\delta^{18}O$ composition at J11 had changed from the pre-melt value of −12.75‰ to −16.65‰ and remained within the aforementioned J11 range until mid-

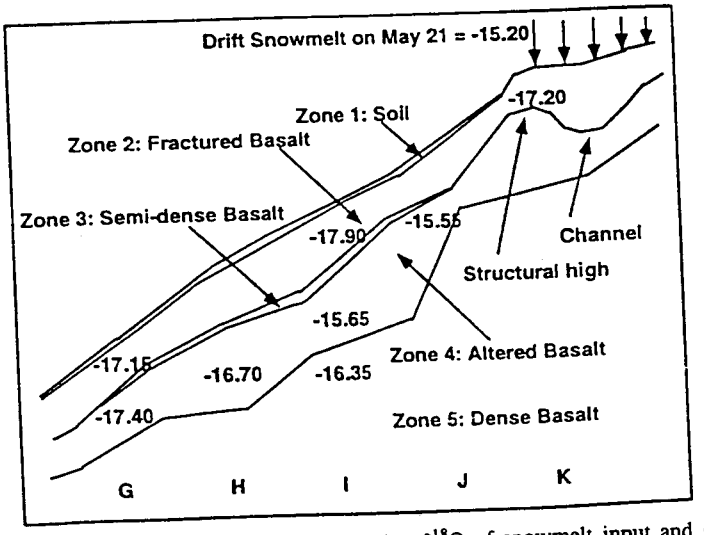

Fig. 5 Schematic cross section showing $\delta^{18}O$ of snowmelt input and geologic zone waters on May 21.

July. Dense basalt $\delta^{18}O$ compositions at I6 and J11 were found to be intermediate between the semi-dense and altered basalt layers. On May 21, dense basalt $\delta^{18}O$ at I6 was $-16.35‰$ (Fig. 5).

DISCUSSION

Subsurface flow mechanisms

Changes in $\delta^{18}O$ downslope from the main drift seem to indicate that the isotopically enriched snowmelt flowed preferentially through the altered basalt (zone 4). This is evidenced by the enriched isotopic composition in zone 4 (similar to drift snowmelt composition) near the base of the drift, that became progressively depleted at locations further downslope towards the stream. Each of these downslope locations retained a distinct isotopic composition within a narrow band throughout the snowmelt season indicating sequential mixing of the enriched meltwater with depleted water previously stored at that location (Fig. 5). Despite continual addition of enriched snowmelt into the altered basalt zone, the downslope isotopic compositions did not show much variation during the study period, indicating the presence of large midslope storages of water. The study of Stevens (1991) showed a relatively large V-shaped depression at midslope location I8 in the cross section of the altered basalt zone which could provide sufficient storage to account for the observed results.

Basinwide snowmelt during the second half of March appears to account for depleted fractured and semi-dense basalt zone compositions (zones 2 and 3). The high G6 snowmelt rates and associated depleted $\delta^{18}O$ values around $-18.00‰$ (Fig. 3) show that subsequent enriched non-drift melt during April was not sufficient to change the isotopic composition of this zone substantially. Enriched $\delta^{18}O$ input from drift snowmelt also did not alter the isotopic composition of the semi-dense and fractured basalt zones. This indicates that the meltwater from the drift largely bypassed the fractured and semi-dense basalt zones and flowed directly into the altered basalt zone. The sharp contrast in the isotopic compositions of fractured and altered basalt zones precludes the possibility of significant exchange of water between them. The isotopic composition indicates some presence and movement of water within the dense basalt zone through small fractures. The water table response seen in this zone may reflect water leaking from the upper altered basalt zone along the sides of deep basalt zone piezometers. However, such a leakage would have lead to $\delta^{18}O$ of the dense basalt zone becoming equal to that of the altered basalt zone, which was not observed.

The close correspondence between $\delta^{18}O$ values of stream and altered basalt zone waters at transect 7 suggests that they are in hydrologic contact. This could be related to positive upward hydraulic gradients and the fact that weathering of the semi-dense basalt layer in the stream channel has made it possible for the underlying altered basalt zone water to rise through this layer and flow into the stream.

Implications for hydrologic modelling

Based on the results of this study, the limitations to modelling water flow using topography driven concepts (e.g. TOPMODEL, Beven & Kirkby, 1979; Tarboton *et al.*,

1995) become apparent. Piezometric data indicate the existence of multiple water tables in the underlying geologic zones. Differences in hydraulic conductivity result in unequal rates of water being transferred downslope through the different zones. There appears to be an effective decoupling of the high conductivity fractured and altered basalt zones (Winkelmaier, 1987) by the presence of the intervening semi-dense basalt zone. Isotopic data suggest that the absence or highly fractured nature of the semi-dense basalt zone under the snow drift location (Fig. 2) causes direct recharge of drift snowmelt into the altered basalt zone, largely bypassing the fractured and semi-dense basalt zones. Within this altered basalt zone, water flow occurs under both phreatic and confined conditions. Approximating the resulting hydraulic gradients using the topographic slope alone could introduce significant differences in the amounts of water conveyed to the stream. A further assumption in the topography based model that saturated hydraulic conductivity decreases exponentially with depth is inappropriate at this site, given the existence of a finite band of high hydraulic conductivity represented by the altered basalt zone.

Preferential flow through the altered basalt has important implications on the moisture available for evapotranspiration. Soil depths around the basin have been described as ranging from 0.3 to 0.6 m (Stevens, 1991). Moisture input into the soil is primarily from basinwide snowmelt and precipitation. Some of this water seeps into the underlying fractured basalt zone where further infiltration is inhibited by the semi-dense basalt zone. Vegetation derives moisture from the soil, with deep roots potentially tapping water in the fractured basalt. Snowmelt water from the main drift flows through the lower altered basalt zone and remains unavailable for the evapotranspiration process due to the intervening semi-dense basalt layer. This results in a decoupling between the water in the fractured basalt and altered basalt zones, which in turn introduces a limit for moisture available for evapotranspiration.

Acknowledgements This work was funded in part by the United States Geological Survey, Department of the Interior, under USGS Grant no. 14-08-0001-G2110. The views and conclusions are those of the authors and should not be interpreted as necessarily representing the official policies, either expressed or implied, of the US Government. The authors are also thankful for the support and contributions by the USDA-ARS Northwest Watershed Research Center, Boise, Idaho. In particular, we thank Dr Keith Cooley, Dr Gerald Flerchinger and Mr Dave Robertson for their help throughout the study. We also thank Dr Hannah Green for help with the final corrections.

REFERENCES

Beven, K. J. & Kirkby, M. J. (1979) A physically-based variable contributing area model of basin hydrology. *Hydrol. Sci. Bull.* **24**(1), 43-69.

Buttle, J. M. (1994) Isotope hydrograph separations and rapid delivery of pre-event water from drainage basins. *Progr. Phys. Geogr.* **18**(1), 16-41.

Flerchinger, G. N., Cooley, K. R. & Ralston, D. R. (1992) Groundwater response to snowmelt in a mountainous watershed. *J. Hydrol.* **133**, 293-311.

Harris, D. M., McDonnell, J. J. & Rodhe, A. (1995) Hydrograph separation using continuous open system isotope mixing. *Wat. Resour. Res.* **31**(1), 157-171.

Maloszewski, P. & Zuber, A. (1993) Principles and practice of calibration and validation of mathematical models for the interpretation of environmental tracer data in aquifers. *Adv. in Wat. Resour.* **16**, 173-190.

McDonnell, J. J. (1990) A rationale for old water discharge through macropores in a steep, humid catchment. *Wat. Resour. Res.* **26**, 2821-2832.

Mock, N. A. (1988) A hydrological characterization of a zero-order basin in volcanic hillslope terrain. Masters Thesis, Dept of Civil & Environ. Engng, Utah State Univ., USA.

Pearce, A. J., Stewart, M. K. & Sklash, M. G. (1986) Storm runoff generation in humid, headwater catchments 1. Where does the water come from? *Wat. Resour. Res.* **22**, 1263-1272.

Sklash, M. G. & Farvolden, R. N. (1979) The role of groundwater in storm runoff. *J. Hydrol.* **43**, 45-65.

Stevens, G. R. (1991) A geophysical investigation of the Upper Sheep drainage, Reynolds Creek Experimental Watershed, Owyhee County, Idaho. Masters Thesis, Univ. of Idaho, USA.

Tarboton, D. G., Jackson, T. H., Liu, J. Z., Neale C. M. U., Cooley, K. R. & McDonnell, J. J. (1995) A grid based distributed hydrologic model: testing against data from Reynolds Creek experimental watershed. In: *Preprints AMS Conf. on Hydrol.*, 79-84, AMS, Dallas.

Wels, C., Cornett, J. R. & Lazerte, B. D. (1993) Hydrograph separation: a comparison of geochemical and isotopic tracers. *J. Hydrol.* **122**, 253-274.

Winkelmaier, J. R. (1987) Groundwater flow characteristics in fractured basalt in a zero-order basin. Masters Thesis, Univ. of Idaho, USA.